A failure analysis of the micromechanisms of fracture of carbon fibre and glass fibre composites in monotonic loading

PETER W. R. BEAUMONT, PAUL D. ANSTICE
Department of Engineering, University of Cambridge, Trumpington Street, Cambridge, UK

The micromechanisms of crack extension of carbon fibres, glass fibres and hybrid composites containing glass fibres and carbon fibres in epoxy and polyester resins have been studied. A new collection of failure data based on observations of fibres debonding, snapping and pulling out has been summarized in cumulative probability diagrams and analysed using Weibull distribution parameters. This data, together with models of failure processes and information of work of fracture, is used to construct fracture-mechanism diagrams. These diagrams, together with the Weibull parameters may help in distinguishing between mechanisms of fracture, give guidance in selecting a material system and in isolating aging and environmental effects.

1. Introduction

In designing structural components from brittle materials, we assume that the operating stress does not exceed the strength of the material for an acceptable level of survival probability. Unfortunately, it is not so straightforward. The probability of failure will be affected by a variety of phenomena; for quasi-brittle fibrous composites, they include premature fracture of the fibres, and slow crack growth in the matrix and at fibre—matrix interfaces. The level of stress required to initiate breakage of a fibre or failure of an interface depends upon the nature of the defect or flaw, its size and the way it interacts with the surrounding microstructure. For example, a weak fibre may fracture at a low stress but not propagate due to some localized plastic flow in the matrix. On the other hand, a small void at an interface or between two adjacent plies in a laminate may extend with ease along the length of the fibre. To complicate matters further, modes of failure are likely to be affected by environment and stress-state.

To have confidence in the design approach where working stress does not exceed ultimate strength for a permissable survival probability, therefore, requires information of the statistics of fracture and a detailed understanding of the micromechanisms of fracture of the material.

If a bar of quasi-brittle fibrous composite is pulled in tension, it may fail in one (or more) of several ways. It may, for example, fracture across the section and produce a flat surface analogous to cleavage fracture in metals. Alternatively, it may fail by the propagation of a crack from one fracture plane to another producing a rough fibrous surface. If the composite is in the form of a laminate, it may fail by delamination and splitting, the precise mode of fracture and direction of crack growth depending upon the orientation of fibres and stacking geometry of the lamellae. At the microscopic level, fibres may debond, fracture at weak points below or on the fracture plane of the matrix, and pull-out. These micromechanisms of fracture occur in a zone surrounding the crack front which we call a microfracture damage zone. It is the work done in creating this damage zone which we equate with the toughness of the composite. The distance over which the fibre debonds and pulls out will depend on a number of intrinsic variables for example fibre—matrix bond strength, distribution of flaws in the fibre. A single composite, glass fibres in epoxy, for instance can show

all these modes of failure. It would be useful to have some idea of the conditions under which each appears for example the effect of intrinsic variables such as surface treatment of the fibre and ductility of matrix, and extrinsic variables, changes in temperature and humidity.

This problem can be tackled in two complementary ways. The range of dominance of the more easily recognized mechanisms, fibre pull-out for instance, can be determined by experiment. A change in temperature or humidity, or the passing of time in a given experiment, in which each mechanism appears can be noted.

Alternatively, one might attempt to couple our understanding of the micromechanisms of cracking with models for each fracture process, and thereby predict the influence of bond strength or toughness of a matrix on each mode of failure. To do so requires some way of quantifying fracture.

Models to describe the various micromechanisms of fracture in quasi-brittle fibrous composites have been described [1–5].

This paper describes the statistical analysis of the micromechanisms of fracture of glass fibres and carbon fibres in polyester and epoxy, and mixtures of the two kinds of fibre in hybrid composites. Considerable failure data, based on the debonded and pulled out lengths of fibre, has been collected in fracture experiments and presented in cumulative probability diagrams.

A statistical analysis of the failure data is then carried out in order to obtain a characteristic value of the debonded and pulled out lengths of fibre for each fibre composite. Three mechanisms are briefly described by which these fibrous composites may fail, using the sequence in which they may occur. An equation is selected for each mechanism, based on a physically sound microscopic model, to describe each failure process in terms of the energy dissipated.

Each equation is then used, together with a value of fibre debond length and fibre pull-out length, to account for the fracture toughness of the composite, and the dominant mechanism of toughening is apparent. Some work of fracture data in this paper are taken from previously published work [1, 2].

2. Failure analysis of fibre debond length and fibre pull-out length

The procedure is as follows: First, the available work of fracture data for the given material is assembled. Then a large amount of fractographic information on fibre–matrix debonding and fibre pull-out process is tabulated. Each failure model is used in turn, together with the failure data to estimate the energy dissipated by the fracture mechanisms.

2.1. Method of collecting failure data

There are, at least, two methods of collecting fractographic information. The first, and most common procedure, is to use a scanning electron microscope for observing fibres protruding above the fracture plane of the matrix. Several areas of the fracture surface are examined, photographs are taken and measurements of a few hundred pulled out fibres are made. However, using this technique, nothing is learned about the fibre–matrix debonding process. A second technique involves the use of an optical microscope and the fracture of model fibrous composites. Such model composites can be in the form of a prismatic bar of transparent resin containing a single layer of unidirectional fibre tape. These have been described previously [1]. The beam is loaded in three-point bending and the layer of fibres is subjected to a tensile stress. Bundles of glass fibres and carbon fibres can be arranged in various ways to produce a series of composites ranging from a glass fibre composite to a carbon fibre composite, with many combinations between the two extremes. These model composites can be thought of as single lamina from which the laminate is made.

The area under the load/displacement curve is equated to the work required to fracture the composite. Tracings are made of each debonded fibre region and each protruding bundle of fibres, observed in transmitted and reflected light, respectively, using an optical microscope [1]. Average values of the *longest* fibres extracted from a matrix and distances over which separation at the fibre–matrix interface have occurred are determined as follows. The area of each tracing is measured using a planimeter and is divided by the width of the fibre bundle. A summation of these values for each bundle is then made and divided by the total number of fibres in the bundles. For example, in specimens containing 5 strands of fibres, (where a strand contains 1 600 individual glass filaments or 5 000 individual carbon filaments), and where 20 tests have been carried out, 400 tracings are made of pulled out fibres and debonded fibres, since the two halves of each speci-

men can be viewed from both sides. Several hundred values of fibre debond length and fibre pull-out length can be made in this way which are then tabulated.

There are, of course, difficulties and ambiguities in a fractographic analysis of this sort. There is the assumption that the profile of the fibre debonded region does not change through the thickness of the bundle of fibres. Turning the test-piece over and examining from both sides will check this. A normal distribution of pulled out lengths of fibre from zero is assumed, where the fibre breaks on the fracture plane of the matrix, and the maximum pull-out length is lp. The average fibre pull-out length is therefore $lp/2$. It is also assumed that each fibre is extracted from its matrix socket without the attachment of fragments of resin onto the surface.

2.2. Statistical analysis of failure data

The statistical prediction of failure relies on the characterization of a flaw strength distribution function [6]. One form of the extreme value distribution is

$$S = \exp{(-\sigma/\sigma_0)}^m V, \qquad (1)$$

where S is the probability of survival, σ is an applied stress on a specimen of volume V, and m and σ_0 are the extreme value distribution parameters. The variability of a set of data decreases as m increases; m and σ_0 therefore characterize the material for prediction of structural reliability. displacement of data for $N = 8000$ fibres. Metallographic examination of various specimens showed excellent penetration of the fibres with resin and the idea that poor wetting of the fibres is responsible for the movement of data to higher values is not correct.

The extreme value distribution equation can describe each set of data. The parameters m and l_0 are determined by replotting the data in logarithmic form, (Fig. 3). Presenting data in this way is useful for characterizing modes of failure and for observing the subtle effects of environment e.g. moisture, on values of m and l_0.

Combining Equation 5 with values of m and l_0 enables us to determine the mean length of debonded and pulled out fibres. Table I lists values of m, l_0 and $\bar{l}$ for the debonding and pulling out of glass fibres in epoxy. For comparison, values of the arithmetic mean of fibre debond length and fibre pull-out length are shown alongside $\bar{l}$ calculated using Equation 5.

Some glass fibre–epoxy specimens were stored at 18 (± 2)° C, 65% relative humidity for 6 months before testing. The distance over which the fibres debonded and pulled out are shown in cumulative probability diagrams (Figs. 4 and 5). Aging the composite has resulted in the data being displaced to lower values of debonding. The inference is that aging, by whatever process, has increased the strength of the glass fibre–epoxy bond with a corresponding decrease in the distance over which the fibre debonds. It may be that additional curing and cross-linking of the resin with time is responsible for improvement in bonding, the effect of the matrix contracting around the fibres. If this is true, then an increase in bond strength, together with a decrease in fibre debond length would result in a fall in toughness of the composite (see Section 3.1). The measured work of fracture of glass fibre in epoxy is $316\,kJ\,m^{-2}$, approximately, and $200\,kJ\,m^{-2}$ after storing for 6 months. In contrast, the pulling out of debonded glass fibres is unaffected by aging (Fig. 5). The distribution of values of pulled out fibres is dependent only on the flaw population of the fibre.

Fractographic information of glass fibres in a glass fibre/carbon fibre/epoxy hybrid is summarized in the following cumulative probability diagrams (Figs. 6 to 8). The fibre debond length data do not superimpose, and increasing the ratio of glass fibres to carbon fibres may displace the data to the right or to the left of the diagram (Fig. 6). For example, increasing the glass fibre content from 30 vol% to 56 vol% of the total fibre content shifts the data from low values to high values; increasing the glass fibre content by a further 7 vol% moves the data back to lower values. Closer examination of the data shows the subtle effects of microstructure on the position of the cumulative probability curve. These effects will be referred to later.

In logarithmic form, Equation 1 can be written

$$\ln{(-\ln S)} = m(\ln \sigma - \ln \sigma_0); \quad (V = 1), (2)$$

where m is the gradient of a linear plot of $\ln{(-\ln S)}$ and $\ln \sigma$, and $\sigma = \sigma_0$ when $S = e^{-1} = 0.37$.

Each mechanism of failure in a fibre composite is affected by the statistical aspects of fibre–matrix bond strength, fibre strength and the distribution of weak points along the length of fibre. This is why a broken fibre composite has a variability of lengths of fibres protruding above the

fracture surface. A quantitative assessment of failure therefore requires a statistical analysis of the micromechanisms of fracture; fibre pull-out length, for example, is likely to be affected by the distribution and strength of weak flaws along the length of the fibre. Equation 1 can be written in terms of the probability of a fibre debonding or pulling out over a particular distance, l,

$$P = 1 - \exp\left(-l/l_0\right)^m, \qquad (3)$$

where $P = 1 - S$.

The mean value, $\bar{l}$, of a distribution of data in the form of Equation 3 can be expressed as

$$\bar{l} = \int_{l_1}^{l_n} (l \, dP/dl) \, dl. \qquad (4)$$

For the case of an extreme value distribution, the mean value, $\bar{l}$, can be expressed

$$\bar{l} = \int_{l_1}^{l_n} m \, (l/l_0)^m \exp\left[-(l/l_0)^m\right] \, dl. \qquad (5)$$

2.3. Cumulative probability diagrams summarizing failure data

Cumulative probability diagrams can summarize a considerable amount of fractographic information on fibre—matrix debonding and fibre pull-out. They show a distribution of extreme values of fibre lengths and by presenting the data in logarithmic form, values of m and l_0 can be determined. These parameters, together with Equation 5 are used to determine values of $\bar{l}$ for fibre debonding and fibre pull-out.

Fig. 1 shows cumulative probability versus fibre debond length, l_d, for model composites containing glass fibres in epoxy. The data does not overlap but are displaced slightly to higher values of l_d as the number of fibres increases. It seems that the debonding process is sensitive to the number of glass fibres in the resin. It is interesting to note, (although it is not obvious why), the data for $N = 4800$ fibres falls to the right of the data for $N = 6400$ fibres. This apparent reversal in trend in the shift of cumulative probability data will be referred to later when we discuss fracture energy. A similar shift of data towards higher fibre lengths is observed for pulled out glass fibres (Fig. 2). The apparent oddity in this case is the disproportionate displacement of data for $N = 8000$ fibres. Metallographic examination of various specimens showed excellent penetration of the fibres with resin and the idea that poor wetting of the fibres is responsible for the movement of data to higher values is not correct.

The extreme value distribution equation can describe each set of data. The parameters m and l_0 are determined by replotting the data in logarithmic form, (Fig. 3). Presenting data in this way is useful for characterizing modes of failure and for observing the subtle effects of environment e.g. moisture, on values of m and l_0.

Combining Equation 5 with values of m and l_0 enables us to determine the mean length of debonded and pulled out fibres. Table I lists values of m, l_0 and $\bar{l}$ for the debonding and pulling out of
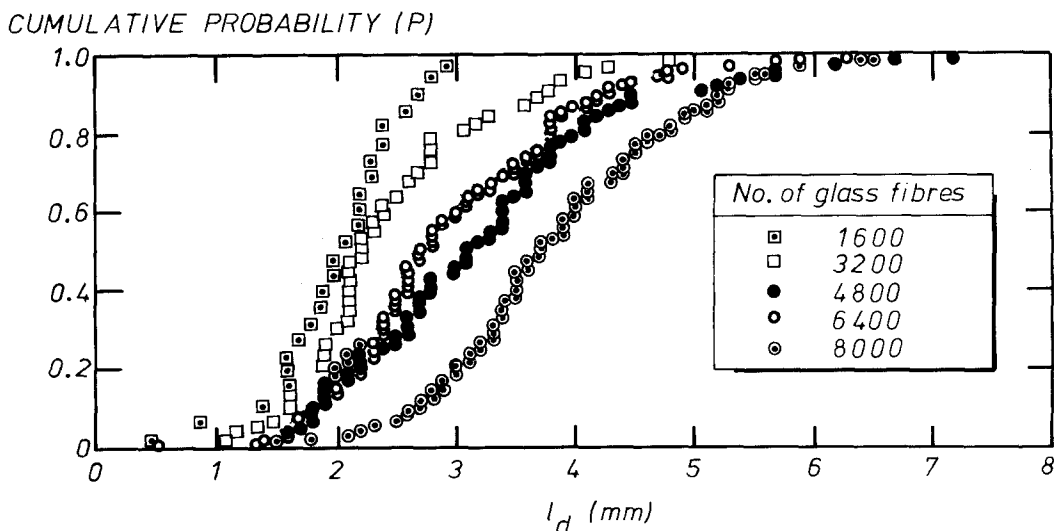

Figure 1 Extreme value distributions of lengths of debonded glass fibres in epoxy for different numbers of strands in the model specimens. (1 strand contains 1600 filaments, 2 strands contains 3200 filaments, and so forth.)
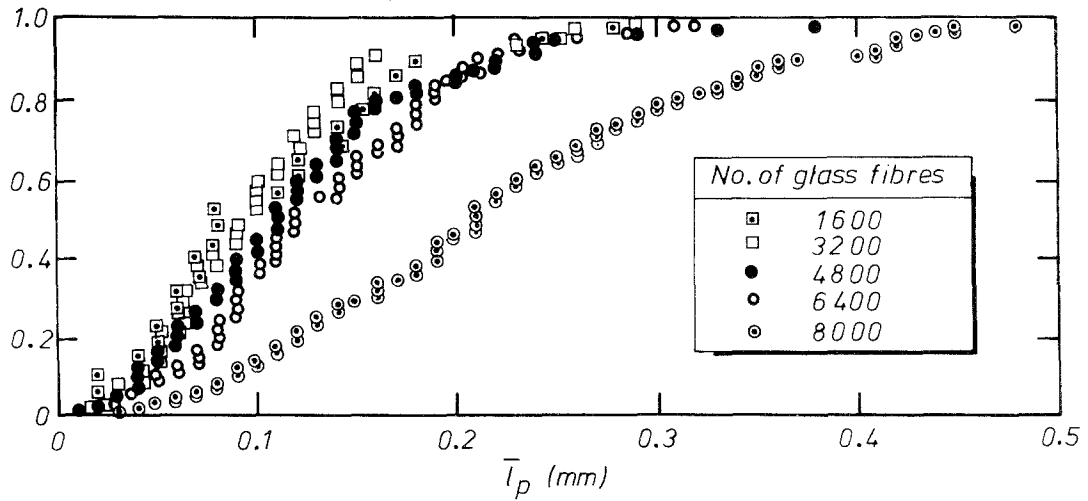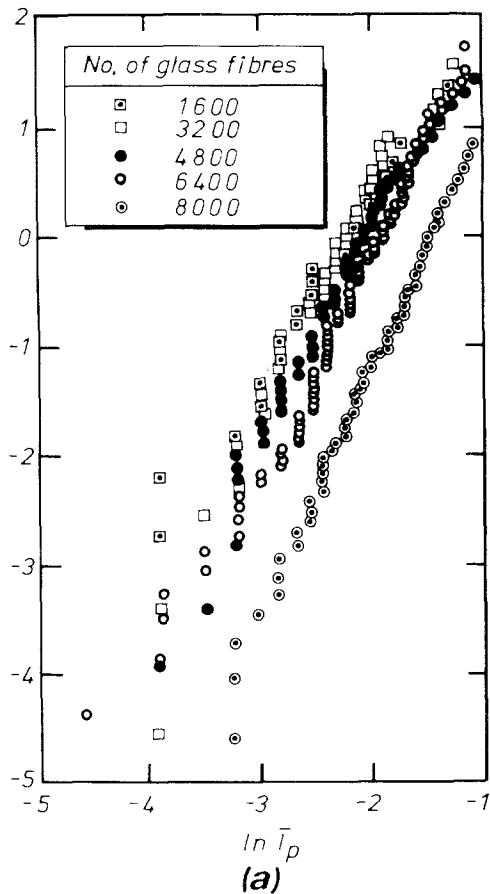
CUMULATIVE PROBABILITY (P)

Figure 2 Extreme value distributions of lengths of pulled out glass fibres in epoxy.
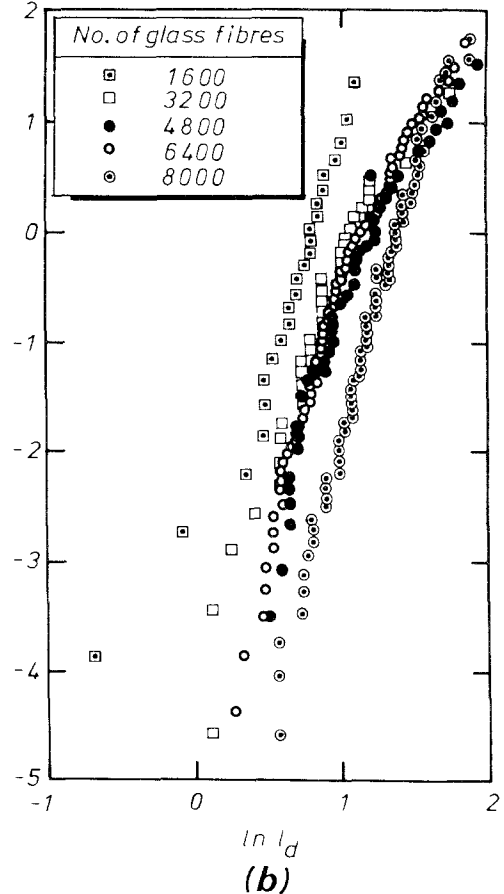

(a)

(b)

Figure 3 Logarithmic plots of the data presented in Figs. 1 and 2.

TABLE I A summary of m, l_0, and $\bar{l}$ for glass fibres in epoxy resin

No. of glass fibre rovings	Fibre debond length (mm)				Fibre pull-out length (mm)			
	m	l_0	$\bar{l}$ (equation 5)	$\bar{l}$ (arithmetic)	m	l_0	$\bar{l}$ (equation 5)	$\bar{l}$ (arithmetic)
1	3.1	2.3	1.7	2.0	1.5	0.12	0.09	0.11
2	3.6	2.7	2.4	2.5	2.0	0.11	0.10	0.11
3	3.1	3.6	3.2	3.2	1.9	0.14	0.13	0.13
4	3.5	3.3	3.0	3.0	1.9	0.15	0.13	0.13
5	4.6	4.2	3.8	3.9	2.2	0.25	0.22	0.24

glass fibres in epoxy. For comparison, values of the arithmetic mean of fibre debond length and fibre pull-out length are shown alongside $\bar{l}$ calculated using Equation 5.

Some glass fibre–epoxy specimens were stored at $18 (\pm 2)^\circ$ C, 65% relative humidity for 6 months before testing. The distance over which the fibres debonded and pulled out are shown in cumulative probability diagrams (Figs 4 and 5). Aging the composite has resulted in the data being displaced to lower values of debonding. The inference is that aging, by whatever process, has increased the strength of the glass fibre–epoxy bond with a corresponding decrease in the distance over which the fibre debonds. It may be that additional curing and cross-linking of the resin with time is responsible for improvement in bonding, the effect of the matrix contracting around the fibres. If this is true, then an increase in bond strength, together with a decrease in fibre debond length would result in a fall in toughness of the composite (see Section

3.1). The measured work of fracture of glass fibre in epoxy is $316 \, \mathrm{kJ \, m^{-2}}$, approximately, and $200 \, \mathrm{kJ \, m^{-2}}$ after storing for 6 months. In contrast, the pulling out of debonded glass fibres is unaffected by aging (Fig. 5). The distribution of values of pulled out fibres is dependent only on the flaw population of the fibre.

Fractographic information of glass fibres in a glass fibre/carbon fibre/epoxy hybrid is summarized in the following cumulative probability diagrams (Figs 6 to 8). The fibre debond length data do not superimpose, and increasing the ratio of glass fibres to carbon fibres may displace the data to the right or to the left of the diagram (Fig. 6). For example, increasing the glass fibre content from 30 vol% to 56 vol% of the total fibre content shifts the data from low values to high values; increasing the glass fibre content by a further 7 vol% moves the data back to lower vlaues. Closer examination of the data shows the subtle effects of microstructure on the position of the cumulative
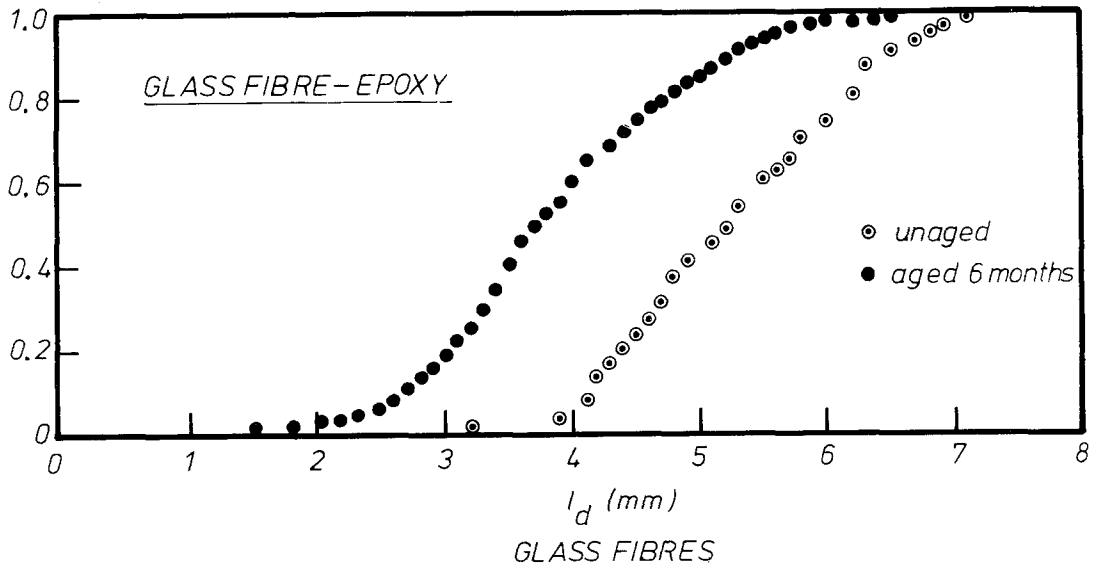

Figure 4 Extreme value distribution of lengths of debonded glass fibres in epoxy before and after aging for 6 months at $18 (\pm 2)^\circ$ C, 65% relative humidity.
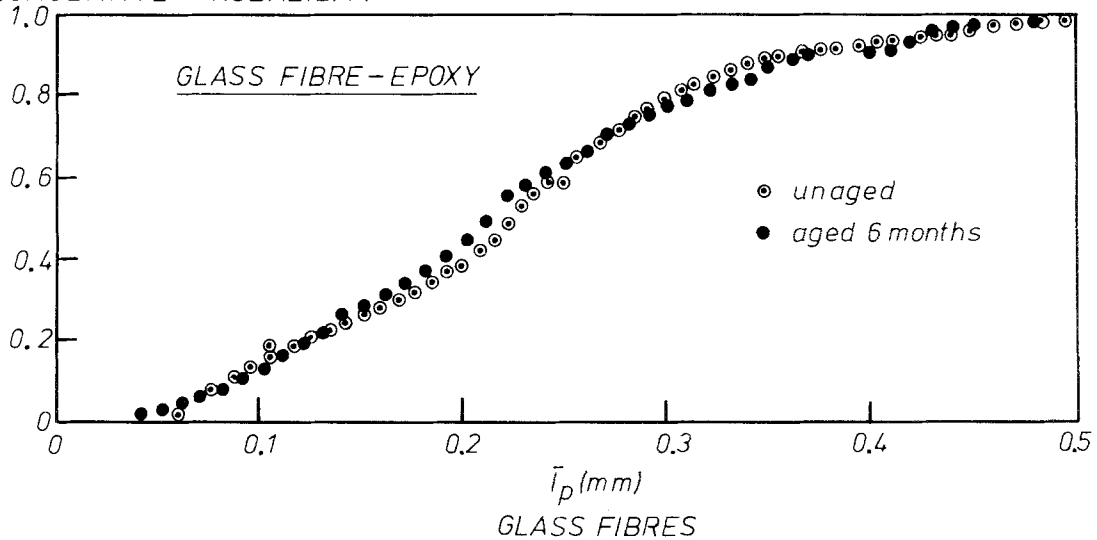
CUMULATIVE PROBABILITY

GLASS FIBRE – EPOXY

⊙ unaged
● aged 6 months

$\bar{l}_p$ (mm)

GLASS FIBRES

Figure 5 Extreme value distribution of lengths of pulled out glass fibres in epoxy before and after aging for 6 months at 18 (± 2)° C, 65% relative humidity.

probability curve. These effects will be referred to later.

In contrast, data of glass fibre pull-out length in the hybrid composite are almost superimposed (Fig. 7). The same applies to the data for carbon fibres (Fig. 8). Each cumulative probability curve overlaps one another and the shape and position of the curves are not significantly affected by variations in composition. The same data plotted in a logarithmic form, based on Equation 2, is used to determine values of m and l_0 (Table II).

Fig. 9 shows the distribution of glass fibre de-

bond lengths as a function of the microstructure of a glass fibre/carbon fibre/polyester hybrid. As we observed and reported earlier, the position of the extreme value distribution depends upon the ratio of carbon fibres to glass fibres. Closer examination of the two diagrams (Figs. 6 and 9) indicates that the relationship between the extreme value distribution and composition is not clear; the movement of cumulative probability curves as the ratio changes is not consistent from one hybrid to the other. In the case of glass fibres in epoxy (without carbon fibres) the data are on the ex-
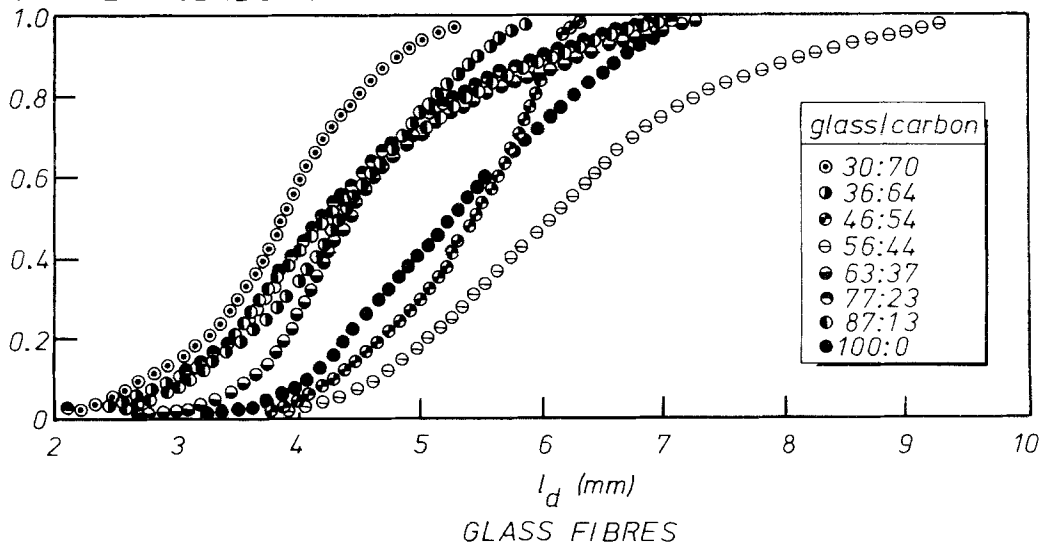
CUMULATIVE PROBABILITY

glass/carbon
⊙ 30:70
◐ 36:64
◕ 46:54
⊖ 56:44
◒ 63:37
◓ 77:23
◖ 87:13
● 100:0

l_d (mm)

GLASS FIBRES

Figure 6 Extreme value distribution of lengths of debonded glass fibres in hybrid composites (epoxy matrix).
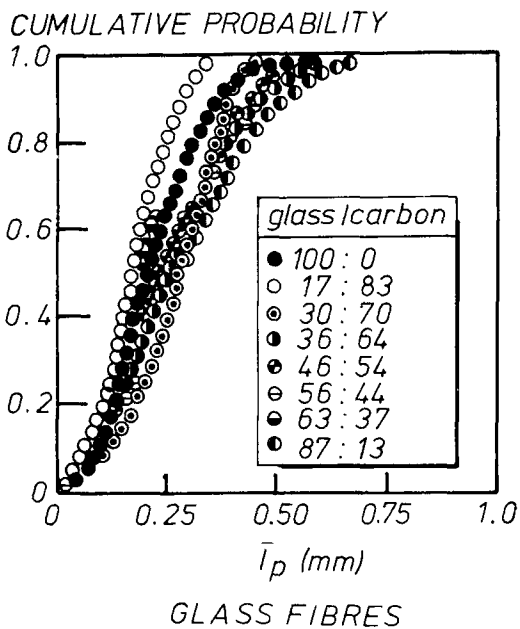
CUMULATIVE PROBABILITY

GLASS FIBRES

Figure 7 Extreme value distribution of lengths of pulled out glass fibre in hybrid composites (epoxy matrix).

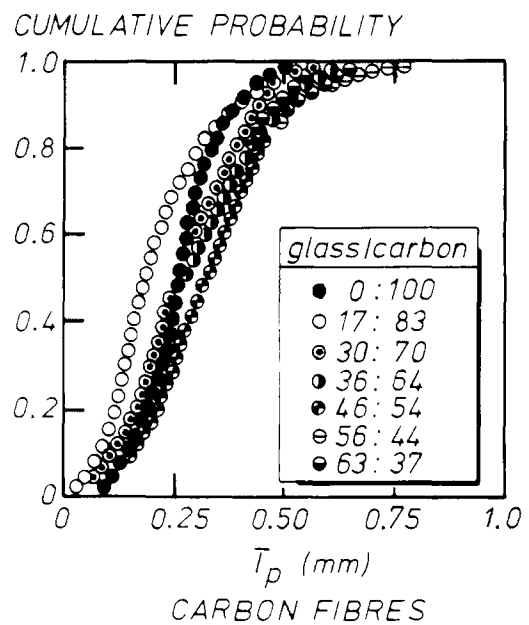CUMULATIVE PROBABILITY

CARBON FIBRES

Figure 8 Extreme value distribution of lengths of pulled out carbon fibres in hybrid composites (epoxy matrix).

treme right of the diagram, while for the polyester composite, the data are towards the extreme left. The pull-out lengths of glass fibres and carbon fibres remain essentially independent of micro-structure (Figs. 10 and 11).

Values of m, l_0 and $\bar{l}$ for the polyester hybrid composites are listed in Table III. In the case of the debonding of glass fibres, m values are slightly higher for epoxy than polyester, while l_0 values are essentially independent of the choice of matrix.

For the extraction of broken glass fibres from their matrix sockets, values of m are similar for the

two resins, while l_0 values are slightly higher for the polyester. In the pulling out of carbon fibres, values of m and l_0 are less for the epoxy than polyester. The indication is that the interfacial bond strength between fibre and matrix is greater for the epoxy composite and, as we shall see later, the toughness is correspondingly lower.

3. Analysis of micromechanisms of fracture based on direct observation

In previous papers [1–5], simple models are derived to describe various mechanisms of fracture of brittle fibrous composites. For convenience, three

TABLE II Values of m, l_0, and $\bar{l}$ for glass fibres and carbon fibres in epoxy resin

Ratio of $C:G$	Glass fibres debonding (mm)			Glass fibres pulling out (mm)			Carbon fibres pulling out (mm)		
	m	l_0	$\bar{l}$	m	l_0	$\bar{l}$	m	l_0	$\bar{l}$
0;100	6.9	5.6	5.3	2.4	0.26	0.23	–	–	–
13:87	4.5	4.9	4.4	2.0	0.36	0.25	1.3	0.35	0.32
23:77	4.2	4.9	4.4	2.1	0.24	0.22	2.0	0.31	0.28
37:63	5.3	5.1	4.7	1.6	0.24	0.23	2.0	0.37	0.32
44:56	5.8	6.7	5.9	1.8	0.32	0.27	2.4	0.30	0.33
54:46	9.1	5.6	5.3	1.7	0.30	0.26	2.6	0.39	0.34
64:36	4.8	4.7	4.3	1.9	0.31	0.27	2.2	0.34	0.31
70:30	5.0	4.1	3.8	2.2	0.31	0.28	2.2	0.32	0.28
83:17	–	–	2.3	3.4	0.21	0.19	2.2	0.25	0.22
100:0	–	–	–	–	–	–	2.4	0.31	0.28

*For glass fibres we have used $\sigma_f = 1.65\,\mathrm{GN\,m^{-2}}$; $E_f = 70\,\mathrm{GN\,m^{-2}}$; $\epsilon_f = 0.01$; and for carbon fibres $\sigma_f = 2.4\,\mathrm{GN\,m^{-2}}$ and $E_f = 240\,\mathrm{GN\,m^{-2}}$.
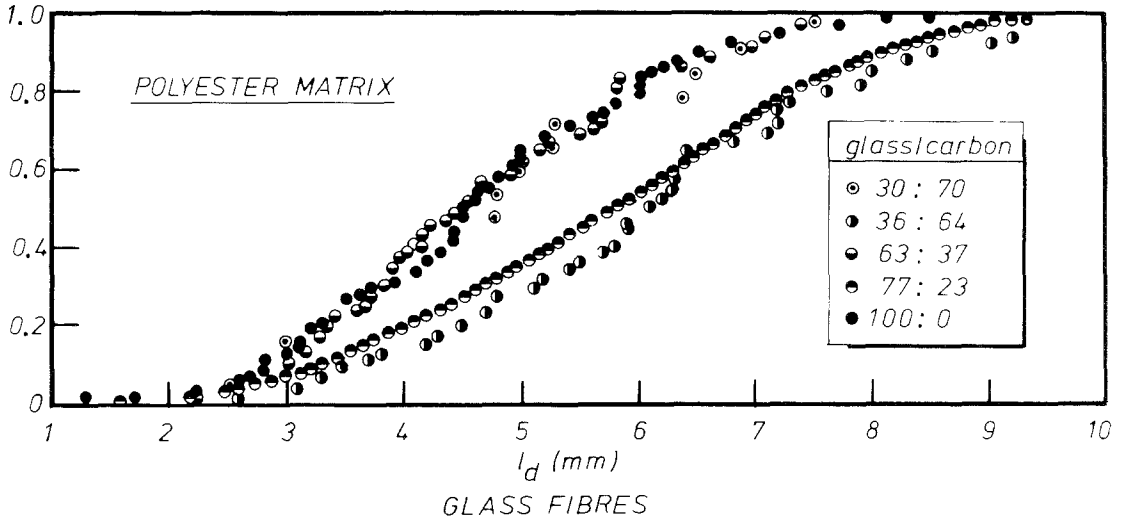
Figure 9 Extreme value distributions of debonded lengths of glass fibres in hybrid composites (polyester matrix).

models, (Fig. 12), together with equations, are listed below

$$W_{pdf} = \pi d\tau \, l_d^2 \, \Delta\epsilon/2 \text{ (post-debond fibre}$$

$$\text{sliding energy);} \qquad (6)$$

$$W_d = \pi d^2 \, \sigma_f^2 \, l_d/8E_f \text{ (fibre deformation energy);}$$
$$(7)$$

$$W_p = \pi d \, \tau l_p^2/6 \text{ (fibre pull-out energy).} \quad (8)$$

(The difference between the strain to failure of fibre and matrix is given by $\Delta\epsilon = \epsilon_f - \epsilon_m$, where $\epsilon_m \simeq 0$ for a brittle, precracked matrix).

The frictional shear stress, τ, which appears in the above relationships can be estimated using the expression [1]

$$\tau = \sigma_f \, d/2 \, l_c. \qquad (9)$$

In a fibre pull-out experiment, the maximum
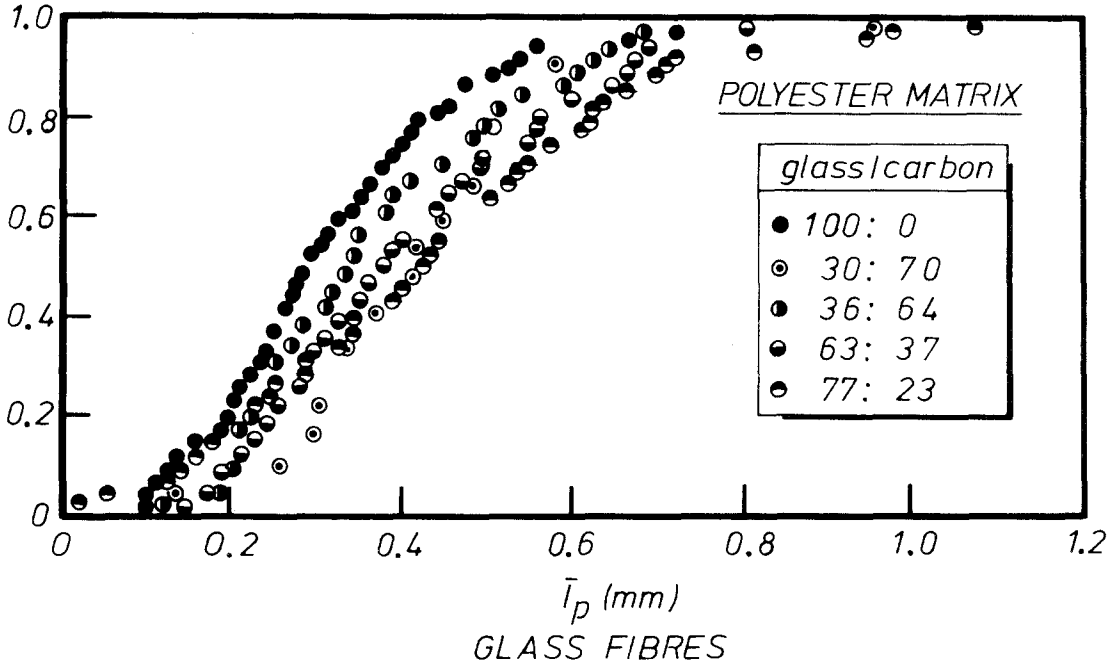
Figure 10 Extreme value distributions of pulled out lengths of glass fibres in hybrid composites (polyester matrix).
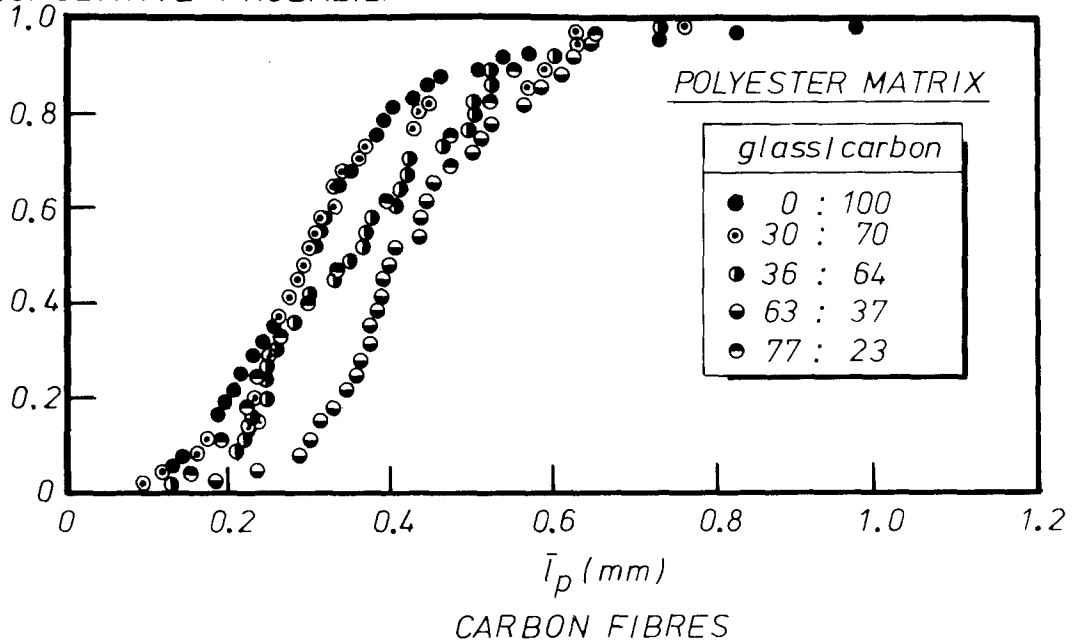
2627

CUMULATIVE PROBABILITY

Figure 11 Extreme value distribution of pulled out lengths of carbon fibres in hybrid composites (polyester matrix).

length of fibre that can be extracted from a block of matrix without first breaking is equal to $l_c/2$. Equations 6 and 8 can be rewritten, therefore, in terms of l_d and l_p

$$W_{pdf} = (\pi d^2 \sigma_f \epsilon_f/8)(l_d^2/l_p); \quad (10)$$

$$+ W_p = \pi d^2 \sigma_f l_p/24, \quad (11)$$

In each model, the work done is directly proportional to the number of fibres and each mechanism, in its own way, is sensitive to the interfacial shear strength. From the above relationships, we can identify three contributions to the total work required to fracture the composite. The total work required to fracture the composite can be written, therefore, in terms of l_d and l_p

$$W_T = N(\pi d^2/48) [(3\sigma_f\epsilon_f)(l_d^2/\bar{l}_p)$$
$$+ (6\sigma_f^2 l_d/E_f) + (4\sigma_f\bar{l}_p)], \quad (12)$$

where l_d is the distance over which the fibre has debonded, $\bar{l}_p$ is the average fibre pull-out length and N is the number of fibres. Therefore, the total work required to fracture a composite can be estimated from a knowledge of the failure parameters of the fibre $\sigma_f, \epsilon_f, l_d$ and l_p.

The characteristic lengths of debonded and pulled out fibres, typical values for σ_f and ϵ_f^*, together with the expressions of fracture energy, are used to estimate the energy dissipated for each mechanism of failure and the total theoretical fracture energy of the composite. Diagrams have been constructed of fracture energy versus number of
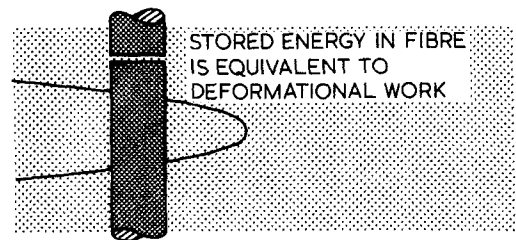
TABLE III Values of m, l_0, and $\bar{l}$ for carbon fibres and glass fibres in polyester resin

Ratio of C : G	Glass fibres debonding (mm)			Glass fibres pulling out (mm)			Carbon fibres pulling out (mm)		
	m	l_0	$\bar{l}$	m	l_0	$\bar{l}$	m	l_0	$\bar{l}$
0:100	3.6	5.2	4.7	2.5	0.35	0.31	—	—	—
23:77	3.4	6.6	5.8	2.0	0.53	0.45	2.7	0.42	0.37
37:63	4.1	5.1	4.7	2.7	0.46	0.41	4.2	0.48	0.44
64:36	4.0	6.7	6.0	2.8	0.41	0.37	3.0	0.42	0.37
70:30	3.7	5.3	4.7	2.5	0.49	0.43	2.6	0.38	0.34
100:0	—	—	—	—	—	—	2.7	0.37	0.33

FRICTIONAL FORCES OPPOSE FIBRE-MATRIX SLIDING

(a)

$$W_{pdf} = \frac{\pi d}{2} \tau \, l_d^2 \, \Delta \varepsilon$$

STORED ENERGY IN FIBRE IS EQUIVALENT TO DEFORMATIONAL WORK

(b)

$$W_d = \pi d^2 \sigma_f^2 \, l_d / 8E_f$$

FRICTIONAL FORCES OPPOSE FIBRE PULL-OUT

(c)
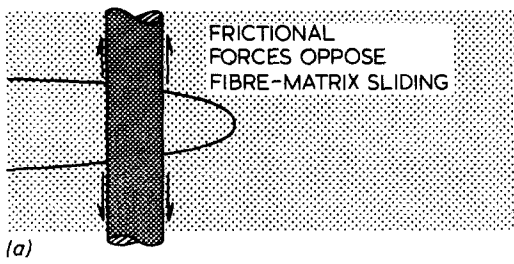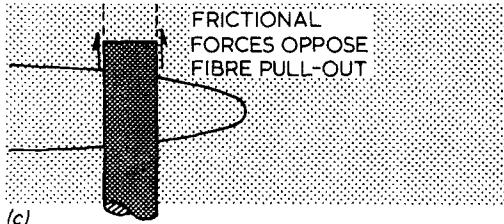
$$W_p = \pi d \tau \, l_p^2 / 6$$

Figure 12 Three micromechanisms of fracture: (a) post-debond fibre sliding; (b) fibre fracture, and (c) fibre pull-out.

fibres for a given composite or proportion of two kinds of fibre for a given hybrid composite system. Since for glass fibres and carbon fibres in brittle polymers, the work of fracture is some 2 to 3 orders of magnitude greater than the work to fracture the matrix, we have chosen to normalize our work of fracture values with cross-sectional area of the fibres. In this way, direct comparison between the models of fracture and experiment can be made.

3.1. Glass fibres in epoxy

A fracture energy diagram for glass fibres in epoxy (Fig. 13a) shows the estimated energy dissipated during the post-debond fibre sliding mechanism (Equation 10). The relationship is not a simple linear one as one would expect from the form of the equation, the cumulative probability data showed fibre debond length to be sensitive to the number of fibres in the composite. It is the square of the fibre debond length and number of fibres which appears in the post-debond fibre sliding equation. The plateau to the curve reflects the reversal in the trend in shift of cumulative probability data for $N = 6400$ fibres to which reference was made earlier.

An estimation of the fibre deformational energy (Equation 7) is shown in the next diagram (Fig. 13b). At first sight, the shape is linear but closer examination shows a smooth curve with a gradu-

ally increasing slope. It reflects the dependence of fibre debond length on the number of glass fibre strands. The plateau shown in the previous figure is less obvious since fibre deformational energy is directly proportional to the length of debonded fibre. The energy dissipated in this way is significantly less than the work done in the post-debond fibre sliding mechanism.

The work to pull broken glass fibres out of a cracked matrix (Equation 11) is of similar order of magnitude as the fibre deformational energy (Fig. 13c). Both diagrams have a similar shape; the increase in gradient of the curve at the high numbers of fibres originates from the high values of fibre pull-out length shown previously in the cumulative probability data for $N = 8000$ fibres.

The result of summing these 3 energy parameters (Equation 12) is shown in Fig. 13d. Apart from a small rise in the curve at $N = 5000$ fibres, approximately, it is a smooth curve with a gradually increasing slope as the number of fibres increases. Comparison of the empirical diagram with experimental work of fracture data shows remarkable likeness in shape and magnitude (Fig. 13e). From observations of the fracture of glass fibres in epoxy we know that the composite exhibits all the common modes of failure; matrix cracking, fibres debonding, fibres snapping and fibres pulling out. The dominant toughening mechanism appears to be post-debond sliding between fibre and matrix; the breakage of fibres and the pulling out of the broken fibre ends dissipates similar amounts of energy and together contribute little more than one-quarter of the total fracture energy of the composite.

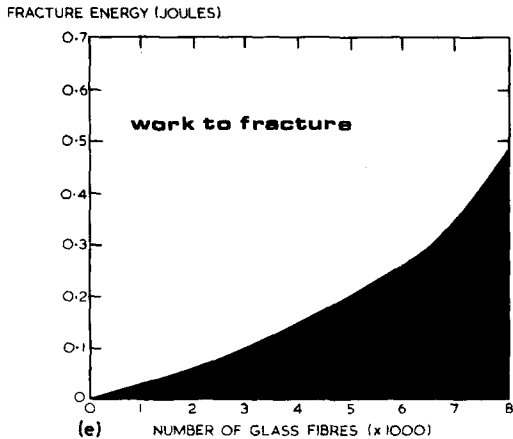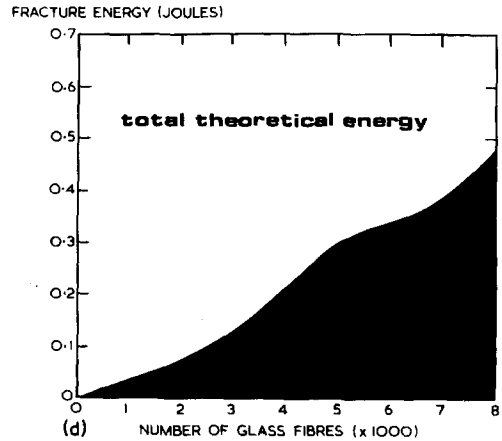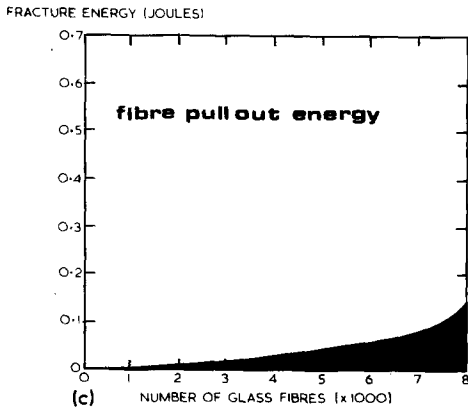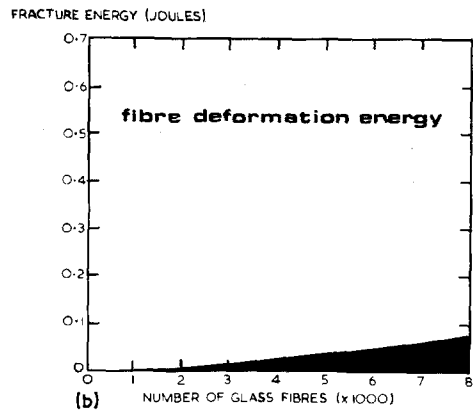Table IV shows the predicted energy terms

FRACTURE ENERGY (JOULES)

post debond sliding energy

(a) NUMBER OF GLASS FIBRES (x 1000)

FRACTURE ENERGY (JOULES)

fibre deformation energy

0·7
0·6
0·5
0·4
0·3
0·2
0·1
0

(b) NUMBER OF GLASS FIBRES (x 1000)

FRACTURE ENERGY (JOULES)

fibre pull out energy

0·7
0·6
0·5
0·4
0·3
0·2
0·1
0

(c) NUMBER OF GLASS FIBRES (x 1000)

FRACTURE ENERGY (JOULES)

total theoretical energy

0·7
0·6
0·5
0·4
0·3
0·2
0·1
0

(d) NUMBER OF GLASS FIBRES (x 1000)

FRACTURE ENERGY (JOULES)

work to fracture

0·7
0·6
0·5
0·4
0·3
0·2
0·1
0

(e) NUMBER OF GLASS FIBRES (x 1000)

Figure 13 Estimations of the energies dissipated for glass fibres in epoxy for each of the three micromechanisms of fracture, based on data of fibre debond length and fibre pull-out length, together with Equations 7, 10, 11, 12.

calculated using the models of fracture, together with characteristic values of debond length and pull-out length of the glass fibres used in the calculation after ageing the composite for 6 months. In the mechanism involving debonding and slippage, ageing has approximately halved the value of the post-debond fibre sliding parameter. The agreement between theoretical energy and experimental work of fracture is a good one.

3.2. Glass fibres and carbon fibres in epoxy

In a similar manner, the work required to fracture a hybrid composite, glass fibres and carbon fibres in epoxy can be estimated. Taking characteristic values of fibre debond length and fibre pull-out length for the glass fibres and carbon fibres, combined with the equations of fracture energy, we can estimate the energy dissipated during fracture and pull-out of both kinds of fibre. In this case, fracture energy is plotted against percentage of carbon fibres in the hybrid composite (Fig. 14).

Fig. 14a shows an estimation of the energy dissipation during glass fibre—matrix sliding soon

	W_{pdf} (kJ m^{-2})	W_d	W_p	W_T	W_{EXPT}
Before aging	215	46	58	319	316
After aging	117	34	58	209	202

These predictions are based on the following measurements: $\bar{l}_d$ (unaged) = 5.3 mm; $\bar{l}_d$ (aged) = 3.9 mm; $\bar{l}_p$ = 0.24 mm approximately, before and after aging. It is the post-debond fibre sliding mechanism and the decrease in $\bar{l}_d$ which appears to be primarily responsible for the decrease in work of fracture.

after the bond has failed. While there is an overall decrease in energy as the carbon fibre content increases, as one would expect, it by no means forms a linear relationship. Certain features are worth pointing out. The first is that after a sharp drop in energy as glass fibre is replaced with carbon fibre, a plateau is observed up to 40 vol% carbon fibre. At this point, the fracture energy actually increases slightly before falling to zero as the remaining glass fibres are replaced with carbon fibres. Recalling the cumulative probability data, it can be realized
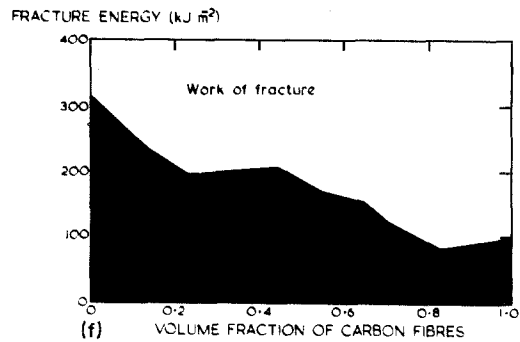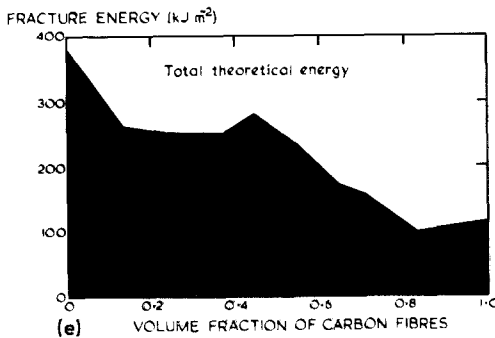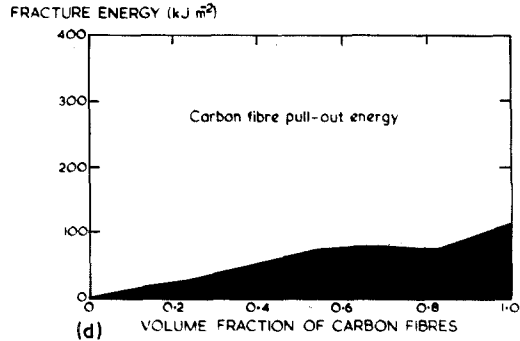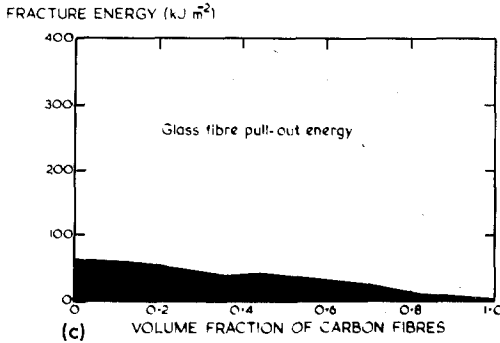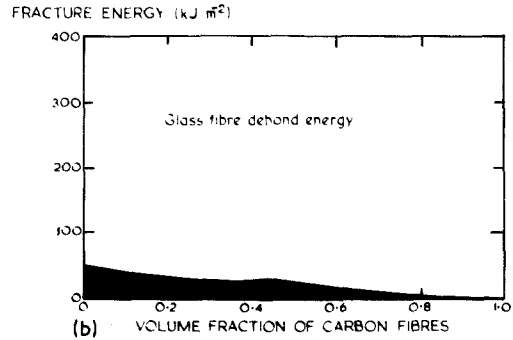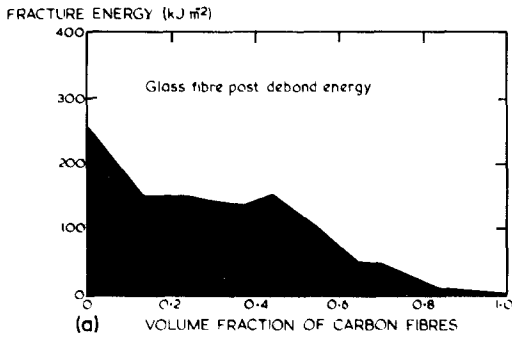

Figure 14 Estimations of the energies dissipated for glass fibres and carbon fibres in epoxy for each of the three micromechanisms of fracture, based on data of fibre debond length and fibre pull-out length, together with Equations 7, 10, 11, 12.
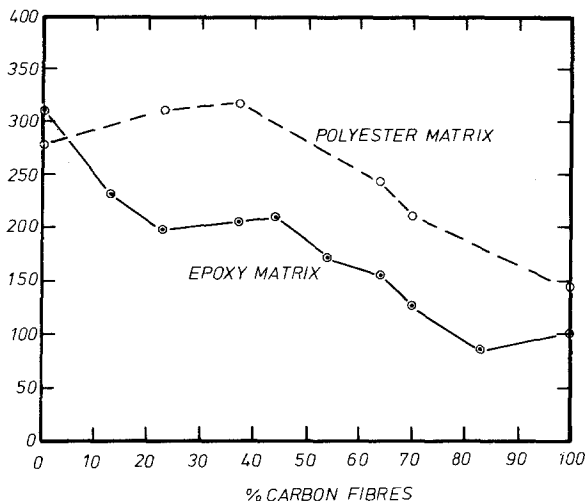
WORK OF FRACTURE
kJ m⁻²

Figure 15 Comparison between experimental work of fracture data of polyester and epoxy hybrid composite systems.

that it is the effects of composition on glass fibre debond length and the subtle balance between debond length and number of fibres which is the origin of the unexpected shape of the post-debond sliding energy diagram. The small peak in the diagram at 44 vol% carbon fibre coincides with the large displacement of the cumulative probability data to higher values of glass fibre debond length.

At first sight, glass fibre deformational energy decreases linearly with an increase in volume fraction of carbon fibre (Fig. 14b). Closer inspection shows a shallow curve with a very small peak at 44 vol% carbon fibre. Minor differences in shape and position of the cumulative probability curves are responsible for the non-linear behaviour.

Slight undulations in the pull-out curve for the glass fibres can also be identified with minor changes in shape and position of the cumulative probability curves. As a first approximation, the glass fibre deformational energy and glass fibre pull-out energy are directly proportional to the amount of glass fibre in the composite, as one would expect from the form of the equations (Figs. 14c and d).

Similar undulations in the carbon fibre pull-out energy diagram originate in small differences to be found in the cumulative probability data. Ignoring these minor effects, the pull-out energy follows a linear relationship with carbon fibre content, as one would expect. Figs. 14e and f show good agreement between theory and experiment.

3.3. Glass fibres and carbon fibres in polyester

In this section, we present work of fracture data of a hybrid system with a polyester matrix. Cumulative probability diagrams showing extreme value distributions of fibre debond lengths and fibre pull-out lengths have been constructed and re-plotted in logarithmic form in order to determine the parameters m and l_0. Data of mean fibre debond length and mean fibre pull-out length, together with the models of micromechanisms of fracture are used to estimate the energies dissipated during crack propagation. Where possible, comparisons are made between the fracture behaviour of the two hybrid systems investigated and the effect of matrix becomes apparent.

Fig. 15 shows the experimental work of fracture data for the two hybrid systems. Certain features of the curves are apparent. First, the general shape of the curves are similar and second, the polyester hybrid composites have work of fracture values which are about 50% higher than values obtained for the epoxy composites. One noticeable exception is the datum point for the glass fibre—polyester; in this case, the work of fracture is less than the value obtained for the epoxy composite. It may be the apparently low value of l_d for glass fibres in polyester that is responsible for the low work of fracture measurement.

Values of debond length and pull-out length for glass fibres and carbon fibres, given in Table III
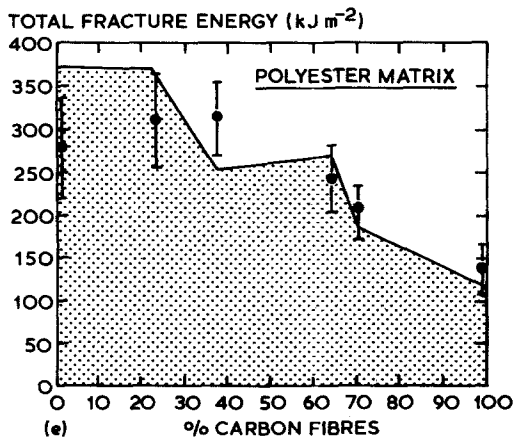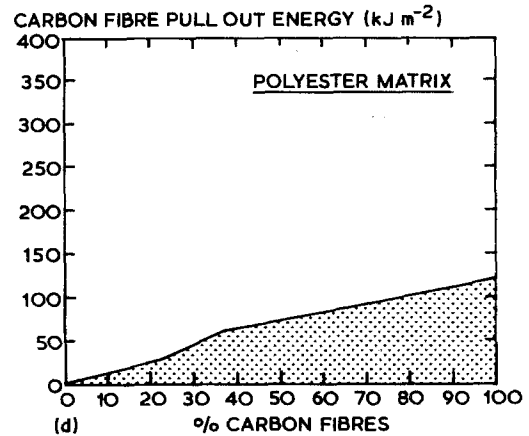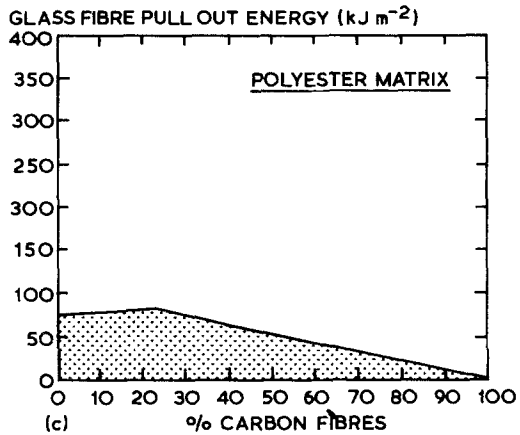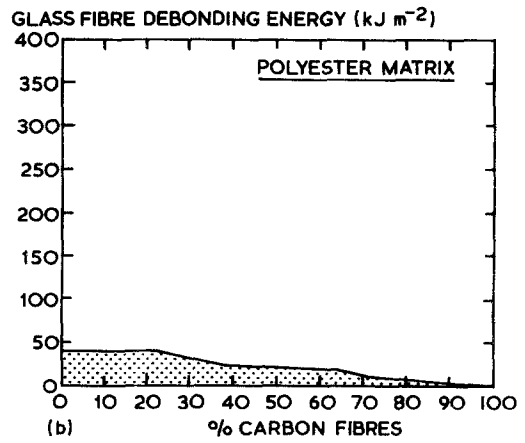
GLASS FIBRE
POST DEBOND SLIDING ENERGY $(kJ\ m^{-2})$

POLYESTER MATRIX

(a) % CARBON FIBRES

GLASS FIBRE DEBONDING ENERGY $(kJ\ m^{-2})$

POLYESTER MATRIX

(b) % CARBON FIBRES

GLASS FIBRE PULL OUT ENERGY $(kJ\ m^{-2})$

POLYESTER MATRIX

(c) % CARBON FIBRES

CARBON FIBRE PULL OUT ENERGY $(kJ\ m^{-2})$

POLYESTER MATRIX

(d) % CARBON FIBRES

TOTAL FRACTURE ENERGY $(kJ\ m^{-2})$

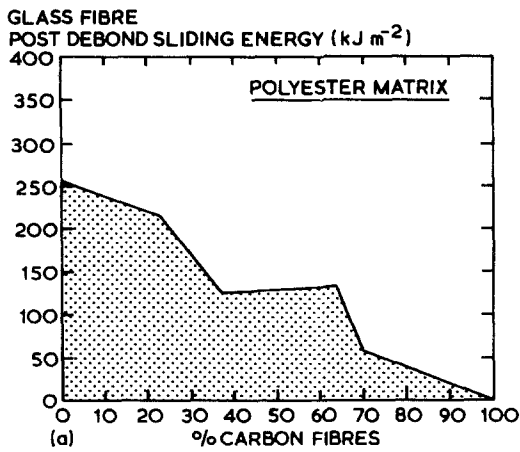POLYESTER MATRIX

(e) % CARBON FIBRES

Figure 16 Estimation of the energies dissipated for glass and carbon fibres in polyester for each of the three micro-mechanisms of fracture, based on data of fibre debond length and fibre pull-out length, together with Equations 7, 10, 11, 12. The points in (e) represent measured work of fracture data.

were used, together with the models of fracture, to predict energies of post-debond fibre sliding, fibre deformational energy, and fibre pull-out. Estimations of these energy parameters for glass fibres and carbon fibres are shown in Fig. 16. Certain comments can be made and generalizations drawn from comparison of the fracture energy diagrams for epoxy and polyester based composites. The overall shapes of the theoretical and experimental fracture energy curves are similar; and the relative order of magnitudes of the four energy parameters and the contribution each one makes to the total fracture energy or toughness of the composite are also alike. The shape of both total theoretical fracture energy curves is dominated by the post-debond fibre sliding term for glass fibres; and at the carbon fibre-rich end of the diagram, the pull-out term for carbon fibres is important. Compari-

2633

TABLE V

Composite	Work of fracture $(kJ\,m^{-2})$
Carbon fibre/epoxy	48
64% carbon fibre/36% glass fibre/epoxy	75
Glass fibre/epoxy	148
Carbon fibre/polyester	70
64% carbon fibre/36% glass fibre/polyester	118
Glass fibre/polyester	132

(The nominal fibre volume fraction is 0.5)

son between the theoretical fracture energy and experimental work of fracture data show remarkable similarities in shape and magnitude. For glass fibres, the post-debond sliding energy term is a major component of the total fracture energy, while the deformational energy and pull-out energy terms are comparable in magnitude. Together, debonding and pull-out of glass fibres contribute no more than one-quarter of the total fracture energy of the hybrid composite. On the other hand, carbon fibres were not observed to debond, and the work in extracting them from a cracked matrix can be successfully equated to the fracture energy of a carbon fibre composite.

4. Work of fracture of structural fibrous composites
Model specimens of the kind used in this study can be used to estimate the work of fracture of structural fibrous composites. Consider, for example, a structural unidirectional glass fibre or carbon fibre composite, fabricated to the dimensions of the model composite, 20 mm × 10 mm × 2 mm. If the fibre volume fraction is 0.5, then the total cross-sectional area of the fibres is 10×10^{-6} m². In a model composite containing 5 tows of carbon fibre, for instance, the total cross-sectional area of the fibres is 1.4×10^{-6} m², approximately. There are about 7 times as many fibres in the structural composite compared to the model composite. If the measured fracture energy of the model carbon fibre composite is multiplied by 7 times, and in the case of the model glass fibre composite containing 5 strands by 8.5 times, the work done in breaking the structural composite can be measured. The work of fracture of the structural composite is calculated by simply dividing the estimated work to break the specimen by twice its cross-sectional area. Table V lists the work of fracture of several

carbon fibre and glass fibre structural composites estimated in this way. They are based on measurements of work of fracture obtained using the model composite specimens. These values are similar to measurements made by others (for example, [7–12]) using fracture mechanics specimens.

5. Summary and implications
When a crack passes through a hybrid composite, the glass fibres are observed to debond and together with the carbon fibres fracture, pulling out of the resin as the surfaces of the matrix crack open. Models based on these observations, predict the energies dissipated when a debonded fibre slides in its socket, snaps and pulls out of the matrix. Detailed comparisons of experimental data combined with the models show that the post-debond fibre sliding mechanism is primarily responsible for the work to fracture glass fibres in epoxy or polyester matrices, while the fibre pull-out mechanism accounts for the fracture energy of carbon fibres in epoxy or polyester resins. It is the subtle balance between these mechanisms and the volume fraction of the carbon fibres and glass fibres in the hybrid composite, and the effects of composition upon the mechanisms of debonding and pull-out where lies the origins of toughness of the hybrid fibre systems.

References
1. J. N. KIRK, M. MUNRO and P. W. R. BEAUMONT, *J. Mater. Sci.* 13 (1978) 2197.
2. M. MUNRO and P. W. R. BEAUMONT, Third International Conference of Mechanical Behaviour of Materials, Cambridge, edited by K. J. Miller and R. F. Smith, (Pergamon Press, Oxford, 1979) 3 253.
3. A. KELLY, *Proc. Roy. Soc.* 319A (1970) 95.
4. P. W. R. BEAUMONT and B. HARRIS, *J. Mater. Sci.* 7 (1972) 1265.
5. B. HARRIS, J. MORLEY and D. C. PHILLIPS, *ibid.* 10 (1975) 2050.

6. A. S. ARGON and F. A. McCLINTOCK, "Mechanical Behaviour of Materials", (Addison–Wesley, Massachusetts 1966).
7. B. HARRIS and A. R. BUNSELL, *Composites* **6** (1975) 197.
8. C. C. CHAMIS, M. P. HANSON and T. T. SERAFINI, *ASTM STP* **497** (1972) 324.
9. R. C. NOVAK and M. A. DeCRESCENTE, *ibid.* **497** (1972) 311.
10. P. W. R. BEAUMONT and D. C. PHILLIPS, *J. Composite Mater.* **6** (1972) 32.
11. J. M. SLEPETZ and L. CARLSON, *ASTM STP* **593** (1974) 143.
12. P. W. R. BEAUMONT and W. L. SERVER, *ibid.* **580** (1975) 443.